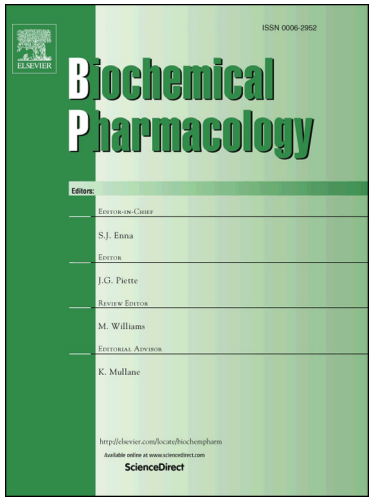

Insight into the role of Urotensin II-Related Peptide Tyrosine residue in UT activation

Etienne Billard, Myriam Létourneau, Terence E. Hébert, David Chatenet

PII: S0006-2952(17)30530-0
DOI: http://dx.doi.org/10.1016/j.bcp.2017.08.003
Reference: BCP 12889

To appear in: *Biochemical Pharmacology*

Received Date: 21 April 2017
Accepted Date: 3 August 2017

Please cite this article as: E. Billard, M. Létourneau, T.E. Hébert, D. Chatenet, Insight into the role of Urotensin II-Related Peptide Tyrosine residue in UT activation, *Biochemical Pharmacology* (2017), doi: http://dx.doi.org/10.1016/j.bcp.2017.08.003

Insight into the role of Urotensin II-Related Peptide Tyrosine residue in UT activation

Etienne Billard[1], Myriam Létourneau[1], Terence E. Hébert[2], David Chatenet[1,*]

[1]INRS – Institut Armand-Frappier, Groupe de Recherche en Ingénierie des Peptides et en Pharmacothérapie (GRIPP), Université du Québec, Ville de Laval, Québec, Canada

[2]Department of Pharmacology and Therapeutics, McGill University, Montréal, Québec, Canada

Correspondance

Dr. David Chatenet, INRS – Institut Armand-Frappier, Groupe de Recherche en Ingénierie des Peptides et en Pharmacothérapie (GRIPP), Université du Québec, Ville de Laval, Québec, Canada. Tel: +1-450-687-5010; Fax: +1-450-686-5446; E-mail address: david.chatenet@iaf.inrs.ca.

Cardiovascular Pharmacology

Abbreviations:

BRET, bioluminescence resonance energy transfer; ACN, acetonitrile; Bip, biphenylalanine; Boc, tert-butoxycarbonyle; BOP, (Benzotriazol-1-yloxy)tris(dimethylamino) phosphonium hexafluorophosphate; CHO cells, Chinese Hamster Ovary cells; DCM, dichloromethane; DIEA, N,N-diisopropylethylamine; DMEM, Dulbecco's Modified Eagle's medium; DMF, dimethylformamide; FBS, foetal bovine serum; Fmoc, Fluorenylmethyloxycarbamate; GFP 10, green fluorescent protein 10; GPCR, G protein-coupled receptor; HEK 293 cells, Human Embryonic Kidney 293 cells; $K_3[Fe(CN)_6]$, potassium ferricyanide; MALDI-TOF, Matrix-assisted laser desorption/ionization-Time of flight; NMR, nuclear magnetic resonance; PAH, pulmonary arterial hypertension; $PdCl_2(PPh_3)_2$, Bis(triphenylphosphine)palladium (II) dichloride; Pep, (phenylethynyl)-phenylalanine; Phe(pI), para-iodo-phenylalanine; Phg, phenylglycine; RlucII, *Renilla* luciferase II; RP-HPLC, Reverse phase-high performance liquid chromatography; Tic(7-OH), 7-hydroxy-1,2,3,4-tetrahydroisoquinoline; Tyr(mI), meta-iodo-tyrosine; UII, Urotensin II; URP, Urotensin II-related peptide; UT, urotensin II receptors.

Abstract

While sharing common biological activity, the two endogenous ligands of the G protein-coupled receptor UT: urotensin II (UII) and urotensin II-related peptide (URP) also exhibit distinct effects, which could be explained by distinct interactions with their cognate receptor (UT). Accordingly, introduction of a similar substitution at the intracyclic Tyr residue in UII and URP led to compounds with divergent pharmacologic profiles. Hypothesizing that the Tyr^6 residue of URP is a key-element to understand the specific activation of UT by URP, we undertook a study of the structure-activity relationship in which this particular residue was replaced by non-natural and constrained amino acids. Each compound was evaluated for its ability to bind UT, to induce rat aortic ring contraction and to activate Gq and G_{12} signalling pathways. We identified [Pep^6]URP, that binds UT with an affinity similar to that of URP, but behaves as a biased ligand. Used as an antagonist, this peptide is also able to selectively reduce the maximal aortic contraction of URP but not UII. Our results suggest that the orientation of the Tyr residue can stabilize at least two different conformations of UT, leading to biased signalling and a probe-dependent allosteric effect.

Keywords: urotensin II-related peptide, human UT, aortic ring bioassay, BRET-based biosensor, bias agonism.

1. Introduction

The urotensinergic system, formed by a G protein-coupled receptor (GPCR) termed UT and two endogenous peptide ligands Urotensin II (UII, H-Glu-Thr-Pro-Asp-[Cys-Phe-Trp-Lys-Tyr-Cys]-Val-OH) and Urotensin II-related peptide (URP, H-Ala-[Cys-Phe-Trp-Lys-Tyr-Cys]-Val-OH), is currently regarded as a potential key contributor to cardiovascular function [1, 2]. Notably, UII is considered one of the most potent endogenous vasoconstrictor and inotropic agents ever described [3, 4]. Over the years, evidence has highlighted the involvement of this system in the genesis and progression of various cardiovascular pathologies including atherosclerosis [5] and pulmonary arterial hypertension (PAH) [6]. Multiple animal studies have shown the therapeutic potential of UT antagonists for treatment of such pathologies but also hypertension, metabolic syndrome, as well as cardiac and renal failure [7-11]. Unfortunately, discrepancies and disappointments were observed with urantide, an antagonist/partial agonist of the urotensinergic system [12], and other candidates as well pointing out a greater need for understanding UT pharmacology at both the molecular and cellular levels.

UII and URP are cyclic peptides that share a common and strictly conserved bioactive cyclic core (-Cys-Phe-Trp-Lys-Tyr-Cys-) but differ by their extracyclic N-terminal residues [4]. Accordingly, while modifications at the N-terminus of UII or URP have almost no impact on their biological activity, several structure-activity relationship analyses, including Ala- and D-scans, revealed that both the nature and orientation of these intracyclic residues were crucial for UT recognition and activation [13-18]. In particular, these studies demonstrated the important role played by the tyrosine residue in UII and URP. For instance, and as recently reported, the

replacement of the Tyr residue with more hydrophobic and/or bulky residues such as (3,4-Cl)Phe or 3-iodo-Tyr as well as the conservation of a specific g^- orientation of the side chain of these residue gave rise to potent UT agonists [19]. While these assumptions are true for UII and its equiactive analog $UII_{(4-11)}$, we currently have limited information regarding the role played by this residue in URP biological activity. UII and URP share common biological actions, however a body of evidence has shown that the two peptides also exert distinct functions, suggesting that these two endogenous UT ligands might be functionally selective [20-24]. As recently demonstrated by virtual docking, the acidic Asp^4 residue of UII or $UII_{(4-11)}$, and not the corresponding aliphatic Ala^1 of URP, can establish a salt bridge with Arg^{193} of the receptor, creating a different binding environment for the two peptides [25]. Supporting this observation, introduction of a Tyr(mI) moiety in $UII_{(4-11)}$ and URP, which only differ by their N-terminal amino acid (Asp versus Ala, respectively), gave rise to two distinct pharmacological profiles with $[Tyr(mI)^6]$URP acting as a weak UT agonist while $[Tyr(mI)^9]UII_{(4-11)}$ is known as a highly potent UT ligand [13, 15]. Such results imply that the Tyr environment in UT may be different for UII and URP following receptor binding. In this context, exploiting this apparent divergence between UII and URP could represent a good opportunity to understand the subtle and pluridimensional pharmacology of UT.

In order to generate insight into the mechanisms of UT recognition and activation by URP, we initiated a structure-activity relationship study at the Tyr^6 position of URP by introducing highly hindered and/or conformationally constrained amino-acids (Figure 1). Compounds were pharmacologically evaluated for their ability 1) to bind UT, 2) to induce/modulate rat aortic ring contraction and 3) to promote activation of Gq and G_{12} using bioluminescence resonance energy transfer (BRET)-based biosensors. The identification of a biased agonist, *i.e.* $[Pep^6]$URP, reveals

a crucial role of this residue in the fine tuning of UT signaling. Furthermore, the ability of this compound to selectively reduce maximal contractile response to URP but not UII indicates that substitution at position 6 could open up new vistas for development of allosteric modulators specifically targeting URP functions.

2. Material and Methods

2.1. Materials

The fluorenylmethyloxycarbamate- (Fmoc-) protected amino-acids, Fmoc-Val-Wang resin and (Benzotriazol-1-yloxy)tris(dimethylamino)phosphonium hexafluorophosphate (BOP) were purchased from Chem-Impex (Wood Dale, IL). Trifluoroacetic acid (TFA), methanol (MeOH), acetonitrile (ACN), diethyl ether, N,N-dimethylformamide (DMF), piperidine and dichloromethane (DCM) were obtained from Fisher Scientific (Nepean, ON). $Na^{125}I$ was purchased from Perkin-Elmer (Montreal, QC). All other chemicals were from Sigma-Aldrich (Mississauga, ON).

2.2. Peptide Synthesis

Peptides were prepared by solid-phase peptide synthesis using a Fmoc protection strategy and a commercially available Fmoc-Val-Wang resin 0.62 meq/g. All reactions were conducted under a nitrogen atmosphere. Fmoc deprotection was achieved with 20% piperidine in DMF for 15 min. Washes were performed with DMF (2x), MeOH (2x) and DCM (2x). Coupling of the Fmoc-protected amino-acids (3-equivalent excess based on the original resin substitution) were mediated by BOP (3 eq) and N,N-diisopropylethylamine (DIEA; 6 eq) in DMF for

approximately 1 h. Completion of the coupling and deprotection steps was monitored with the qualitative Kaiser test. The phenylacetylenyl side chain was introduced on Boc-[L/D-Phe(pI)^{6}]URP peptidyl-resins using the Sonogashira cross-coupling reaction and a previously reported procedure [20]. Briefly, a solution of DMF/DCM (50/50) is added to the peptidyl-resin (1 eq) and the mixture was degassed in the reactor with nitrogen 15 min prior to the reaction. Then, phenylacetylene (3 eq), Bis(triphenylphosphine)palladium (II) dichloride ($PdCl_2(PPh_3)_2$; 0.1 eq), copper iodide (CuI; 0.1 eq), tricyclohexylphosphine (0.2 eq) and triethylamine (3 eq) were added into the reaction vessel and the reaction mixture was then agitated through nitrogen bubbling overnight at room temperature (RT). The resin was then washed with DMF (2x), 0.1 M diethyldithiocarbamate in DMF (2x, 5 min) in order to remove the excess of Pd-catalyst, DMF (2x), MeOH (2x), and DCM (2x). All peptides were cleaved from their solid support with concomitant side-chain deprotection by exposing the peptidyl-resin to a mixture of trifluoroacetic acid containing water (2.5%), ethanedithiol (2.5%) and triisopropylsilane (1%) for 3 h at RT. The filtrate was evaporated and the crude peptide was precipitated with diethylether. In most cases, disulfide bridge formation was achieved through the iodine oxidation method as previously described [26]. However, for alkyne-containing peptides, cyclization was induced by dissolving the crude peptide in an aqueous solution of acetonitrile (50/50; v/v) at a concentration of 1 mg/mL. Then, the pH was raised to 8 with a diluted solution of ammonium hydroxide prior to the addition of potassium ferricyanide ($K_3[Fe(CN)_6]$; 2 eq). The mixture was stirred for 3 h and the pH was then adjusted to 3.5 with acetic acid. Purification of peptides was achieved by RP-HPLC using a X-Terra-Prep MS© C_{18} column and a linear gradient of 0-100% eluant B (50 % acetonitrile in 0.06% water) over 2 h. Peptide homogeneity was evaluated by analytical RP-HPLC (C_{18} CSC-Kromasil column and a linear gradient of 0-60 % of ACN over 30 min) and

MALDI-TOF mass spectrometry (Voyager-DE, sources) in linear mode using α-cyanohydroxycinnamic acid as matrix. Fractions with a purity above 95 % were pooled, lyophilized and stored at -20°C.

2.3. Aortic ring contraction experiments

Adult male Sprague-Dawley rats (Charles-Rivers, San Diego, CA) weighing 250–300 g were housed in group cages under controlled illumination (12:12h light-dark cycle), humidity, and temperature (21-23 °C) and had free access to tap water and rat chow. All experimental procedures were performed in accordance with regulations and ethical guidelines from the Canadian Council for the Care of Laboratory Animals and received approvals of the institutional animal care and use committee of the *Institut National de la Recherche Scientifique-Institut Armand-Frappier*. As previously described [20], the thoracic aorta was cleared of surrounding tissue and then excised from the aortic arch to the diaphragm. Conjunctive tissues were next removed from the thoracic aorta and the vessels were divided into 4 mm rings. The endothelium of each aortic ring was removed by gently rubbing the vessel intimal surface. Aortic rings were then placed in a 5 mL organ bath filled with oxygenated normal Krebs-Henselheit buffer. Eighty microliter of a 2.5 M potassium chloride solution (40 mM final concentration in bath) was used to evaluate the contractile responses of each vessel. Cumulative concentration-response curves to synthetic peptides were obtained by increasing the concentration of each peptide in the organ chamber (3.10^{-11} to 3.10^{-6} M). The amplitude of the contraction induced by each concentration of peptide was expressed as a percentage of the KCl-induced contraction. For antagonist assay, a concentration of 3.10^{-8} M of [Pep^{6}]URP was applied 30 minutes prior treatment with cumulative concentrations of UII or URP (10^{-11} to 10^{-6} M). The median effective concentrations (EC_{50}) are

expressed as the mean ± S.E.M., and the *n* values, representing the total number of animals from which the vessels were isolated, varied from 3-19 animals.

2.4. Ligand Binding

Synthetic URP was radiolabeled with $Na^{125}I$ using the chloramine T technique as previously reported [13]. Iodinated ^{125}I-URP were purified on a C_{18} cartridge, collected and stored at -20ºC until use. Competitive binding experiments were performed using a stable CHO-UT cell line, expressing the human UT isoform (generous gift from Drs H. Vaudry and C. Dubessy, Rouen, France), and as previously described [13]. Briefly, cells plated in 24-well plate at a density of 150,000 cells/well were incubated on ice and for 2h with increasing concentration of various peptides (10^{-11} to 10^{-5} M) in the presence of ^{125}I-URP (0.2 nM). Non-specific binding was established by exposing cells to 10^{-5} M cold URP. Cells were washed twice with cold binding buffer then lysed with a solution of sodium hydroxide (1 M). Cell-bound radioactivity was quantified using a γ-counter. Results were expressed as a percentage of the specific binding of ^{125}I-URP obtained in the absence of competitive ligands.

2.5. Generation of a stable HEK 293-cell line expressing human UT

A pcDNA3.1+ vector containing the human UT receptor cDNA cloned at EcoRI and BamHI restriction sites was obtained from Missouri S & T cDNA Resource Center. HEK 293 cells, grown in DMEM culture media supplemented with 10% foetal bovine serum, HEPES, and sodium pyruvate without antibiotics, were plated in a 6-well plate at 200,000 cells/well and transfected following a $CaCl_2$ procedure [27]. At 48 h post-transfection, cells were trypsinized and G418 (selection antibiotic) was added at 800 µg/mL to culture media. The optimal selection

antibiotic concentration was determined by performing a kill curve assay on HEK 293 cells (data not shown). Cells were cultured under the selection antibiotic for 8-10 days (untransfected cells died within 10 days) with medium changed every 2 days. Positive cells (unaffected by the selection antibiotic) were maintained until they reached 80% confluency. Cells were then trypsinized, diluted and plated in 96-well plates at a very low density (about 1 cell/well) to isolate clones. Cells from single-colony wells were transferred to 6-well plates for expansion. For each clone, presence of UT mRNA was confirmed by RT-PCR and the clone, HEK 293-UT, having the best growing properties was chosen for our subsequent studies.

2.6. Gq and G_{12} activation assays

HEK 293-UT cells were grown in DMEM culture media supplemented with 10% foetal bovine serum, HEPES, sodium pyruvate and G418 (400 µg/mL). Passages were performed when cells reached 80% of confluency. Cells were initially plated in 96-well plates at a density of 10,000 cells/well. The following day, the medium is replaced with DMEM culture media supplemented with 2.5% foetal bovine serum (FBS), and 5 h later, cells were transiently transfected with 0.025 ng/well of a Gq-polycistronic or 0.005 ng/well of a G_{12}-polycistronic BRET sensor [28]. Sixteen hours post-transfection, medium was replaced with DMEM supplemented with 5% FBS, HEPES, sodium pyruvate and G418 (400 µg/mL) and cell growth was resumed for another 24 h. Cells were washed with 120 µL PBS solution supplemented with 0.1 % of glucose, and then incubated with 80 µL of this solution for 2 h. Then, 10 µl of a 1/20 dilution (diluted before use) of coelenterazine 400A (stock at 1 mM in ethanol) in Krebs and 10 µl of the 10x appropriate concentration were added, and the luminescence was evaluated with an Infinite® M1000 PRO. Filters were set at 410 nm and 515 nm for detecting the *Renilla* luciferase II (RlucII, donor) and

green fluorescent protein 10 (GFP10, acceptor) light emission, respectively. BRET signals were monitored for 5 min after co-addition of coelenterazine 400A and ligands. BRET ratio was determined by calculating the ratio of the light emitted by GFP10 over the light emitted by the RlucII. BRET signals were normalized to that of URP (10^{-5}M).

2.7. Statistical analysis

Aortic contraction assays, binding experiments and G-protein activation were performed at least in triplicate. Data, expressed as mean ± S.E.M, were analyzed with the Prism Software (Graphpad Software, San Diego, CA, USA). Sigmoidal dose-response fits with variable slope and one-site competition functions were used to determine EC_{50} and IC_{50}, respectively. Bias between Gq and G_{12} pathways was determined using the ratios of transduction coefficients [29]. Statistical comparisons were analyzed by the Student's t-test, and differences were considered significant where $*P < 0.05$, $**P < 0.01$ or $***P < 0.001$.

3. Results

3.1. Peptide structure and analysis.

Structures of the non-natural amino-acids used in this study are presented in Figure 1. RP-HPLC analysis of URP and related analogs revealed that their purity was higher than 98%. For all peptides, the molecular weight observed by MS analysis agreed with theoretical values (Table 1).

3.2. Binding Affinity of URP and related analogs.

As shown in Table 2, replacement of the Tyr residue with various hydrophobic substituents generated analogs that retained a good binding affinity toward UT (Figure 2). For instance, [Pep^6]URP (pIC_{50} = 7.70 ± 0.09) binds UT much like URP (pIC_{50} = 7.64 ± 0.09). However, [Phe(pI)^6]URP and [Bip^6]URP exhibited a greater binding affinity (pIC_{50} = 8.25** ± 0.10 and pIC_{50} = 8.19 ± 0.12, respectively; $P < 0.01$) than the native ligand (pIC_{50} = 7.64 ± 0.09). In contrast to their L-counterpart, [D-Phe(pI)^6]URP, [D-Bip^6]URP, and [D-Pep^6]URP bound UT with a weak affinity ($pIC_{50} < 6$). Finally, the introduction of constrained amino acids resulted in two compounds, [Tic(7-OH)^6]URP and [Phg^6]URP, which showed reduced binding affinity (pIC_{50} = 6.11 ± 0.11 and 6.45 ± 0.22, respectively).

3.3. Vasocontractile action of URP and related analogs.

Each compound was then evaluated for its propensity to induce aortic ring contraction (Figure 3). While [Phe(pI)^6]URP, [Bip^6]URP, and [Pep^6]URP exhibited a similar or even greater binding affinity compared to URP, these molecules exhibited very different vasoactive profiles (Figure 3, Table 2). For instance, [Pep^6]URP, with a binding affinity similar to that of URP, induced aortic ring contraction with a potency significantly lower (pEC_{50} = 6.77 ± 0.10) than that of URP (pEC_{50} = 8.11 ± 0.06). Surprisingly, [Bip^6]URP, which was a significantly better UT binder than URP, produced a less potent (pEC_{50} = 7.50 ± 0.18) but still efficacious (E_{max} = 105 ± 8%) aortic ring contraction compared to URP (pEC_{50} = 8.11 ± 0.06; E_{max} = 116 ± 4%). Also, [Phe(pI)^6]URP, which possessed a similar binding affinity to [Bip^6]URP, was able, like URP, to potently (pEC_{50} = 8.12 ± 0.20) and efficaciously (E_{max} = 95 ± 7%) induce aortic ring contraction (Figure 3; Table 2). Surprisingly, these results appear to be in contrast with the results obtained in the radioligand binding assays. Compounds, [D-Phe(pI)^6]URP, [D-Bip^6]URP, and [D-Pep^6]URP, retained low to

very low binding affinity also exhibited a weak propensity to induce rat aortic contraction (Figure 3, Table 2). Finally, introduction of a conformational constraint within URP at position 6 produced two partial agonists, eliciting approximately 45% and 30% of the maximal URP-induced contraction (E_{max} = 116 ± 4%), respectively.

3.4. Gq and G_{12} activations.

Discrepancies observed between our binding assays and our aortic ring contraction experiments could be the result of a system bias due to species differences or biased signaling. Since aortic ring contraction is in part mediated by intracellular calcium mobilization following activation of G_q [30] and by the stimulation of the small GTPase RhoA following G_{12} activation [31], we next evaluated the ability of [Phe(pI)^6]URP, [Pep^6]URP, [D-Bip^6]URP, and [Tic(7-OH)^6]URP to recruit G_q using a BRET-based biosensor (Figure 4, Table 3). Treatment of HEK 293-UT cells with [Phe(pI)^6]URP produced G_q activation (pEC_{50} = 7.85 ± 0.17) similar to that observed for URP (pEC_{50} = 8.03 ± 0.18). These results are in accordance with the respective effects exerted by URP and [Phe(pI)^6]URP in our aortic ring experiments. Similarly, [Pep^6]URP (pEC_{50} = 6.84 ± 0.16) and [Tic(7-OH)^6]URP (pEC_{50} = 7.00 ± 0.24) exhibited a lower propensity to activate G_q. Interestingly, while the efficacy of [Pep^6]URP to stimulate G_q signalling was similar to that of URP, [Tic(7-OH)^6]URP was only able to reach 61 ± 7% of the URP-associated G_q activation. [D-Bip^6]URP failed to activate G_q.

We next evaluated the ability of those analogs to activate G_{12}. Except for [D-Bip^6]URP that failed to activate G_{12}, all of them behaved as full agonists with varying potencies (Figure 5, Table 3). While [Pep^6]URP and [Phe(pI)^6]URP produced a similar activation of G_{12} (pEC_{50} = 7.32 ± 0.17; E_{max} = 90 ± 6 and pEC_{50} = 7.57 ± 0.20; E_{max} = 92 ± 6, respectively) compared to

URP (pEC_{50} = 7.43 ± 0.15; E_{max}= 100), [Tic(7-OH)^6]URP-induced G_{12} activation was significantly less potent than URP (pEC_{50} = 6.73 ± 0.18, $*P \leq 0.05$). Bias determination revealed that while [Phe(pI)^6]URP was unbiased (1.51 ± 1.31), [Pep^6]URP (9.95 ± 1.42, $**P \leq 0.01$) and [Tic(7-OH)^6]URP (22.13 ± 1.51, $***P \leq 0.001$) were strongly and significantly biased toward G_{12} compared to URP.

3.5. Antagonistic nature of [Pep^6]URP.

Considering that [Pep^6]URP has a similar affinity than URP but behave as a biased agonist, we investigated its propensity to block hUII- and/or URP-mediated rat aortic contraction as previously reported for several recently developed analogs [20, 21, 32-34]. Tested at 3 X 10^{-8}M, a concentration that only produced 10% contraction, [Pep^6]URP is able to reduce UII contractile potency (pEC_{50} = 8.11 ± 0.12 *vs* 8.52 ± 0.11 no treatment, $*P \leq 0.05$) without affecting its efficacy (Figure 5, Table 4). Surprisingly, this analog significantly diminished both the potency and the efficacy of URP to induce contraction (pEC_{50} = 7.30 ± 0.24, $***P \leq 0.001$; E_{max} = 73 ± 5, $***P \leq 0.001$).

4. Discussion

Several studies have recently shown that UII and URP might indeed be functionally selective UT agonists [20-24, 33, 34]. Over the years, characterization of structure-activity relationships (SAR) have highlighted the crucial role played by the common C-terminal cyclic core of UII and URP in regards to their biological activity [4, 16]. The N-terminal domain of UII was generally deemed unimportant for the function of UII. However, we and others recently demonstrated the existence of an initial interaction between this N-terminal domain, particularly

the glutamic and aspartic acid residues, and the receptor that could lead to specific topological changes associated with UT activation [20, 25]. Accordingly, a recent study suggested that the different biological effects of UII and URP were not caused by differences in ring conformations but rather by different interactions with UT [35]. Since most of the SAR studies have been conducted on UII, SAR studies on URP are rather sparse with limited information regarding UT activation. To date, all SAR studies, conducted on UII, URP or their related analog $UII_{(4\text{-}11)}$, have demonstrated the importance of the aromatic ring at position 6/9 of URP and UII, respectively. Hence, while [Ala^6]URP and [Ala^9]UII exhibited a drastic reduction in binding affinity and biological activity [13, 18], almost all aromatic-substituted UII analogs retained good activity. The present study is the first to explore the impact of various para-substituted phenylalanine moieties on the binding and biological activity of URP.

Except [Phg^6] and [$Tic(7\text{-}OH)^6$]URP, all L-substituted URP analogs at position 6 retained a similar if not better binding affinity than URP, therefore suggesting that, as for UII [15, 18, 36, 37], the presence of an aromatic ring is a major determinant for its binding while the presence of an hydroxyl group is not crucial. Interestingly, the significantly higher affinity of [Bip^6]URP and [$Phe(pI)^6$]URP suggest that the augmentation of the hydrophobicity parameter augment the binding, which is also in line with previous studies [19, 37]. Notably, replacement of the Tyr residue in the UII-related analog, Ac-c[CFWKYC]-NH_2, resulted in a tenfold improvement in binding affinity compared to UII [37]. Other modifications introduced within URP, including isomer substitution or conformational restraint, generated weak UT binders. Since NMR analysis of URP has revealed the presence of a turn structure stabilised by the Tyr^6 residue [13, 25, 38], perturbation of this secondary structure in URP, through side-chain modification/orientation like in [D-Pep^6]URP and [$Tic(7\text{-}OH)^6$]URP, has probably prevented its proper binding to UT.

Overall, while the steric hindrance of the side chain at position 6 does not appear to be a critical parameter, the orientation of those side chains is of paramount importance for proper UT recognition.

On one hand and in accordance with their binding affinity, all D-isomers and conformationally restricted analogs exerted a weak to very weak contractile action. Notably, while all D-isomers acted as very weak agonists, reaching between 7 and 60% of URP maximum response at 10^{-5}M, the two constrained analogs behaved as weak partial agonists (Table 2, Figure 3). On the other hand, all L-substituted URP analogs were full UT agonists, their vasocontractile actions appear correlated with an augmentation of the steric parameter or with the length of the π-electronic cloud of the para-group. Altogether, while the orientation of the side chain is again a negative contributor for biological activity of URP analogs, the length of the substituent in para, which seems to preserve or improve binding affinity, tends to be an unfavorable determinant for their vasocontractile activity. However, as previously reported for UII and its related analogs $UII_{(4-11)}$, substitution of the Tyr residue by bulky aromatic amino acids including (2-naphthyl)-L-alanine, biphenylalanine, and 3-iodo-tyrosine or replacement of the hydroxyl group with various substituents such as $-OCH_3$, $-NO_2$, COOH, and $-NH_2$ increased or left unaffected binding affinity and biological activity through enhancement of the hydrophobic interactions within a putative Tyr binding pocket of UT [36, 37]. Surprisingly, [3-iodo-Tyr^6]URP is characterized by a two-fold decrease in binding affinity and a nine fold decrease in contractile activity [13]. While the common and minimal requirement at this position for UII and URP appeared to be the presence of an aromatic moiety, the introduction of substituted phenylalanine or tyrosine residues in UII and URP yielded distinct results that might suggest a different mode of interaction with UT.

The significant differences observed for [Pep^6]URP between its binding affinity and biological activity could result from inter-species variability, since hUT and rUT share only 75%

of sequence homology [3], or signaling bias. In order to assess this question, we evaluated the propensity of [Phe(pI)^6]URP, [D-Bip^6]URP, [Tic(7-OH)^6]URP and [Pep^6]URP to activate G_q and G_{12} following stimulation of hUT. Using a G_q BRET-based biosensor, the results that we obtained were consistent with those obtained in the rat aortic contraction bioassay, negating the possibility of an interspecies bias. Notably, [Pep^6]URP, which is less potent than URP to induce contraction, was also less potent than URP for triggering Gq activation. Interestingly, [Phe(pI)^6]URP and [Pep^6]URP activated G_{12} with a potency and efficacy similar to that of URP while [D-Bip^6]URP was inactive. The signaling bias observed with [Pep^6]URP on G_{12} over Gq but not [Phe(pI)^6]URP could explain, at least in part, the discrepancies observed in this study between binding affinity and biological activity, those two G proteins being involved in the vasocontractile action of UII and URP.

Tested at a concentration (3 X 10^{-8}M) that does not trigger contraction, [Pep^6]URP behaved as an atypical antagonist exerting a probe-dependent action on UII and URP. On one hand, this analog reduced UII potency to induce contraction without affecting its efficacy. On the other hand, it diminished both URP potency and efficacy. Binding experiments performed in this study suggest that URP and [Pep^6]URP compete to a common binding site, however this probe-dependent mechanism suggests an allosteric mode of action. Due to the high similarity between [Pep^6]URP and URP, it is unlikely that this peptide binds to a site distinct to the orthosteric one. Owing to the traditional view that GPCRs were monomeric, thus non-interacting proteins, allosteric modulators were usually defined as chemical entities that could alter the binding or function of orthosteric ligands by binding the same (monomeric) GPCR at a topographically different binding site [39]. However, allosteric binding sites can also be distinct at the molecular level. Indeed, as described by Kenakin: "Allosterism can be defined as the process by which the

interaction of a chemical or protein at one location on a protein or macromolecular complex (the allosteric site) influences the binding or function of the same or another chemical or protein at a topographically distinct site" [39]. Such a description provides a framework to understand the allosteric nature of GPCR oligomers. Hence, binding of the natural ligand (agonist) to one protomer of the complex is expected to modify, through allosteric communication between protomers, the binding of a second molecule by altering the conformation of the second protomer [39], giving rise to cooperative effects [40]. We therefore believe that [Pep^{6}]URP is indeed working through such a mechanism involving UT homodimers. Supporting our hypothesis, binding experiments suggested the existence of two binding sites with varied affinity for UII in cultured rat astrocytes [23] and recombinant cells expressing human UT receptors [41].

NMR and docking experiments performed with P5U (a potent peptidic UT agonist) and urantide (a peptidic UT antagonist/biased agonist) revealed different orientation of their common Tyr residue [42, 43]. NMR studies driven in membrane-mimicking micelles showed a difference in the orientation of Tyr residue: g^{-} in agonists [17, 25, 44] *versus* trans for antagonists [19, 43]. Urantide, which possesses a Tyr position in trans, has been shown to behave as a partial agonist in G_q activation [30]. In the present study, we showed that [Tic(7-OH)^{6}], which conformation is restricted to g^{+} [45], acted also as a partial agonist, suggesting that a g^{-} conformation of the Tyr is necessary for complete activation of G_q.

Molecular recognition is determined by the structure and dynamics of both a protein and its ligand. The induced fit and conformational selection mechanisms are two models generally used to explain the transition of a GPCR from an unbound conformation to a bound conformation in complex with its ligand. In both models, agonist binding involves the formation and the disruption of intramolecular interactions between chemical substituents on the agonist

and specific amino acids in the GPCR [46]. This process, occurring through kinetically distinct steps involving conformational intermediates, suggests that structurally different ligands will therefore disrupt distinct combinations of stabilizing intramolecular interactions leading ultimately to distinct signaling signature. Thus, the ability of [Pep^6]URP to fully activate G_{12} but not Gq is probably linked to an augmentation of the length in para of the aromatic ring of this residue, creating steric hindrance that probably perturbs molecular microswitches involved in Gq but not G_{12} activation

Taken together, these observations indicate that Tyr^6 represents a complex switch in URP since receptor-binding and agonism-defining determinants are structurally integrated. Strikingly, and in support of our proposed mechanism, similar observations, demonstrating the involvement of agonist switches during the AT1R activation, were reported. This study, apart from suggesting an induced fit mode of activation, indicated that binding and activation of the AT1R by angiotensin II were not interrelated [47]. Finally, [Pep^6]URP represents a new class of derivative that could reduce significantly both the efficacy and the potency of URP without altering the efficacy of hUII. Overall, our study highlights for the first time the crucial role of the Tyr residue of URP in the activation process of UT and suggests that modification at this position could open up new avenue in the design of allosteric modulators of the urotensinergic system.

Conflicts of interest

The authors declare no conflicts of interest.

Acknowledgments

We thank the Canadian Institutes of Health Research (CIHR) and the Natural Sciences and Engineering Research Council of Canada (NSERC) for funding.

References

[1] S.A. Douglas, E.H. Ohlstein, Human urotensin-II, the most potent mammalian vasoconstrictor identified to date, as a therapeutic target for the management of cardiovascular disease, Trends in cardiovascular medicine 10(6) (2000) 229-37.

[2] S.A. Douglas, A.C. Sulpizio, V. Piercy, H.M. Sarau, R.S. Ames, N.V. Aiyar, E.H. Ohlstein, R.N. Willette, Differential vasoconstrictor activity of human urotensin-II in vascular tissue isolated from the rat, mouse, dog, pig, marmoset and cynomolgus monkey, British journal of pharmacology 131(7) (2000) 1262-74.

[3] R.S. Ames, H.M. Sarau, J.K. Chambers, R.N. Willette, N.V. Aiyar, A.M. Romanic, C.S. Louden, J.J. Foley, C.F. Sauermelch, R.W. Coatney, Z. Ao, J. Disa, S.D. Holmes, J.M. Stadel, J.D. Martin, W.S. Liu, G.I. Glover, S. Wilson, D.E. McNulty, C.E. Ellis, N.A. Elshourbagy, U. Shabon, J.J. Trill, D.W. Hay, E.H. Ohlstein, D.J. Bergsma, S.A. Douglas, Human urotensin-II is a potent vasoconstrictor and agonist for the orphan receptor GPR14, Nature 401(6750) (1999) 282-6.

[4] H. Vaudry, J. Leprince, D. Chatenet, A. Fournier, D.G. Lambert, J.C. Le Mevel, E.H. Ohlstein, A. Schwertani, H. Tostivint, D. Vaudry, International Union of Basic and Clinical Pharmacology. XCII. Urotensin II, urotensin II-related peptide, and their receptor: from structure to function, Pharmacological reviews 67(1) (2015) 214-58.

[5] I. Albanese, S.S. Daskalopoulou, B. Yu, Z. You, J. Genest, A. Alsheikh-Ali, A.G. Schwertani, The Urotensin II System and Carotid Atherosclerosis: A Role in Vascular Calcification, Front Pharmacol 7 (2016) 149.

[6] Y. Pehlivan, R. Dokuyucu, T. Demir, D.S. Kaplan, I. Koc, M. Orkmez, I.H. Turkbeyler, A.O. Ceribasi, E. Tutar, S. Taysi, B. Kisacik, A.M. Onat, Palosuran treatment effective as bosentan in the treatment model of pulmonary arterial hypertension, Inflammation 37(4) (2014) 1280-8.

[7] Y.A. Kim, D.G. Lee, K.Y. Yi, B.H. Lee, Y.S. Jung, Blockade of Urotensin II Receptor Prevents Vascular Dysfunction, Biomol Ther (Seoul) 24(5) (2016) 523-8.

[8] H. Krum, W. Kemp, Therapeutic potential of blockade of the urotensin II system in systemic hypertension, Current hypertension reports 9(1) (2007) 53-8.

[9] A.M. Watson, M. Olukman, C. Koulis, Y. Tu, D. Samijono, D. Yuen, C. Lee, D.J. Behm, M.E. Cooper, K.A. Jandeleit-Dahm, A.C. Calkin, T.J. Allen, Urotensin II receptor antagonism confers vasoprotective effects in diabetes associated atherosclerosis: studies in humans and in a mouse model of diabetes, Diabetologia 56(5) (2013) 1155-65.

[10] Z. You, J. Genest, Jr., P.O. Barrette, A. Hafiane, D.J. Behm, P. D'Orleans-Juste, A.G. Schwertani, Genetic and pharmacological manipulation of urotensin II ameliorate the metabolic and atherosclerosis sequalae in mice, Arteriosclerosis, thrombosis, and vascular biology 32(8) (2012) 1809-16.

[11] Z. You, H. Al Kindi, A. Abdul-Karim, P.O. Barrette, A. Schwertani, Blocking the urotensin II receptor pathway ameliorates the metabolic syndrome and improves cardiac function in obese mice, FASEB journal : official publication of the Federation of American Societies for Experimental Biology 28(3) (2014) 1210-20.

[12] R. Patacchini, P. Santicioli, S. Giuliani, P. Grieco, E. Novellino, P. Rovero, C.A. Maggi, Urantide: an ultrapotent urotensin II antagonist peptide in the rat aorta, British journal of pharmacology 140(7) (2003) 1155-8.

[13] D. Chatenet, C. Dubessy, J. Leprince, C. Boularan, L. Carlier, I. Segalas-Milazzo, L. Guilhaudis, H. Oulyadi, D. Davoust, E. Scalbert, B. Pfeiffer, P. Renard, M.C. Tonon, I. Lihrmann, P. Pacaud, H. Vaudry, Structure-activity relationships and structural conformation of a novel urotensin II-related peptide, Peptides 25(10) (2004) 1819-30.

[14] S. Flohr, M. Kurz, E. Kostenis, A. Brkovich, A. Fournier, T. Klabunde, Identification of nonpeptidic urotensin II receptor antagonists by virtual screening based on a pharmacophore model derived from structure-activity relationships and nuclear magnetic resonance studies on urotensin II, Journal of medicinal chemistry 45(9) (2002) 1799-805.

[15] P. Labarrere, D. Chatenet, J. Leprince, C. Marionneau, G. Loirand, M.C. Tonon, C. Dubessy, E. Scalbert, B. Pfeiffer, P. Renard, B. Calas, P. Pacaud, H. Vaudry, Structure-activity relationships of human urotensin II and related analogues on rat aortic ring contraction, Journal of enzyme inhibition and medicinal chemistry 18(2) (2003) 77-88.

[16] J. Leprince, D. Chatenet, C. Dubessy, A. Fournier, B. Pfeiffer, E. Scalbert, P. Renard, P. Pacaud, H. Oulyadi, I. Segalas-Milazzo, L. Guilhaudis, D. Davoust, M.C. Tonon, H. Vaudry, Structure-activity relationships of urotensin II and URP, Peptides 29(5) (2008) 658-73.

[17] A. Carotenuto, L. Auriemma, F. Merlino, A. Limatola, P. Campiglia, I. Gomez-Monterrey, R. di Villa Bianca, D. Brancaccio, P. Santicioli, S. Meini, C.A. Maggi, E. Novellino, P. Grieco, New insight into the binding mode of peptides at urotensin-II receptor by Trp-constrained analogues of P5U and urantide, Journal of peptide science : an official publication of the European Peptide Society 19(5) (2013) 293-300.

[18] A. Brkovic, A. Hattenberger, E. Kostenis, T. Klabunde, S. Flohr, M. Kurz, S. Bourgault, A. Fournier, Functional and binding characterizations of urotensin II-related peptides in human and rat urotensin II-receptor assay, The Journal of pharmacology and experimental therapeutics 306(3) (2003) 1200-9.

[19] A. Carotenuto, L. Auriemma, F. Merlino, A.M. Yousif, D. Marasco, A. Limatola, P. Campiglia, I. Gomez-Monterrey, P. Santicioli, S. Meini, C.A. Maggi, E. Novellino, P. Grieco, Lead optimization of P5U and urantide: discovery of novel potent ligands at the urotensin-II receptor, Journal of medicinal chemistry 57(14) (2014) 5965-74.

[20] D. Chatenet, M. Letourneau, Q.T. Nguyen, N.D. Doan, J. Dupuis, A. Fournier, Discovery of new antagonists aimed at discriminating UII and URP-mediated biological activities: insight into UII and URP receptor activation, British journal of pharmacology 168(4) (2013) 807-21.

[21] D. Chatenet, Q.T. Nguyen, M. Letourneau, J. Dupuis, A. Fournier, Urocontrin, a novel UT receptor ligand with a unique pharmacological profile, Biochemical pharmacology 83(5) (2012) 608-15.

[22] N.D. Doan, T.T. Nguyen, M. Letourneau, K. Turcotte, A. Fournier, D. Chatenet, Biochemical and pharmacological characterization of nuclear urotensin-II binding sites in rat heart, British journal of pharmacology 166(1) (2012) 243-57.

[23] M. Jarry, M. Diallo, C. Lecointre, L. Desrues, T. Tokay, D. Chatenet, J. Leprince, O. Rossi, H. Vaudry, M.C. Tonon, L. Prezeau, H. Castel, P. Gandolfo, The vasoactive peptides urotensin II and urotensin II-related peptide regulate astrocyte activity through common and distinct mechanisms: involvement in cell proliferation, The Biochemical journal 428(1) (2010) 113-24.

[24] H.C. Prosser, M.E. Forster, A.M. Richards, C.J. Pemberton, Urotensin II and urotensin II-related peptide (URP) in cardiac ischemia-reperfusion injury, Peptides 29(5) (2008) 770-7.

[25] D. Brancaccio, F. Merlino, A. Limatola, A.M. Yousif, I. Gomez-Monterrey, P. Campiglia, E. Novellino, P. Grieco, A. Carotenuto, An investigation into the origin of the biased agonism associated with the urotensin II receptor activation, Journal of peptide science : an official publication of the European Peptide Society 21(5) (2015) 392-9.

[26] J. Erchegyi, R. Cescato, C.R. Grace, B. Waser, V. Piccand, D. Hoyer, R. Riek, J.E. Rivier, J.C. Reubi, Novel, potent, and radio-iodinatable somatostatin receptor 1 (sst1) selective analogues, Journal of medicinal chemistry 52(9) (2009) 2733-46.

[27] M. Kwon, B.L. Firestein, DNA transfection: calcium phosphate method, Methods Mol Biol 1018 (2013) 107-10.

[28] B. Breton, E. Sauvageau, J. Zhou, H. Bonin, C. Le Gouill, M. Bouvier, Multiplexing of multicolor bioluminescence resonance energy transfer, Biophys J 99(12) (2010) 4037-46.

[29] T. Kenakin, A. Christopoulos, Signalling bias in new drug discovery: detection, quantification and therapeutic impact, Nat Rev Drug Discov 12(3) (2013) 205-16.

[30] C. Brule, N. Perzo, J.E. Joubert, X. Sainsily, R. Leduc, H. Castel, L. Prezeau, Biased signaling regulates the pleiotropic effects of the urotensin II receptor to modulate its cellular behaviors, FASEB journal : official publication of the Federation of American Societies for Experimental Biology 28(12) (2014) 5148-62.

[31] V. Sauzeau, E. Le Mellionnec, J. Bertoglio, E. Scalbert, P. Pacaud, G. Loirand, Human urotensin II-induced contraction and arterial smooth muscle cell proliferation are mediated by RhoA and Rho-kinase, Circ Res 88(11) (2001) 1102-4.

[32] J. Dufour-Gallant, D. Chatenet, W.D. Lubell, De Novo Conception of Small Molecule Modulators Based on Endogenous Peptide Ligands: Pyrrolodiazepin-2-one gamma-Turn Mimics

That Differentially Modulate Urotensin II Receptor-Mediated Vasoconstriction ex Vivo, Journal of medicinal chemistry 58(11) (2015) 4624-37.

[33] F. Merlino, A.M. Yousif, E. Billard, J. Dufour-Gallant, S. Turcotte, P. Grieco, D. Chatenet, W.D. Lubell, Urotensin II((4-11)) Azasulfuryl Peptides: Synthesis and Biological Activity, Journal of medicinal chemistry 59(10) (2016) 4740-52.

[34] M. Strack, E. Billard, D. Chatenet, W.D. Lubell, Urotensin core mimics that modulate the biological activity of urotensin-II related peptide but not urotensin-II, Bioorg Med Chem Lett (2017).

[35] E. Haensele, N. Mele, M. Miljak, C.M. Read, D.C. Whitley, L. Banting, C. Delepee, J. Sopkova-de Oliveira Santos, A. Lepailleur, R. Bureau, J.W. Essex, T. Clark, Conformation and Dynamics of Human Urotensin II and Urotensin Related Peptide in Aqueous Solution, J Chem Inf Model (2017).

[36] R. Guerrini, V. Camarda, E. Marzola, M. Arduin, G. Calo, M. Spagnol, A. Rizzi, S. Salvadori, D. Regoli, Structure-activity relationship study on human urotensin II, Journal of peptide science : an official publication of the European Peptide Society 11(2) (2005) 85-90.

[37] W.A. Kinney, H.R. Almond Jr, J. Qi, C.E. Smith, R.J. Santulli, L. de Garavilla, P. Andrade-Gordon, D.S. Cho, A.M. Everson, M.A. Feinstein, P.A. Leung, B.E. Maryanoff, Structure-function analysis of urotensin II and its use in the construction of a ligand-receptor working model, Angew Chem Int Ed Engl 41(16) (2002) 2940-4.

[38] E. Lescot, J. Sopkova-de Oliveira Santos, C. Dubessy, H. Oulyadi, A. Lesnard, H. Vaudry, R. Bureau, S. Rault, Definition of new pharmacophores for nonpeptide antagonists of human urotensin-II. Comparison with the 3D-structure of human urotensin-II and URP, J Chem Inf Model 47(2) (2007) 602-12.

[39] T. Kenakin, L.J. Miller, Seven transmembrane receptors as shapeshifting proteins: the impact of allosteric modulation and functional selectivity on new drug discovery, Pharmacological reviews 62(2) (2010) 265-304.

[40] L. Albizu, M.N. Balestre, C. Breton, J.P. Pin, M. Manning, B. Mouillac, C. Barberis, T. Durroux, Probing the existence of G protein-coupled receptor dimers by positive and negative ligand-dependent cooperative binding, Mol Pharmacol 70(5) (2006) 1783-91.

[41] M. Clozel, P. Hess, C. Qiu, S.S. Ding, M. Rey, The urotensin-II receptor antagonist palosuran improves pancreatic and renal function in diabetic rats, The Journal of pharmacology and experimental therapeutics 316(3) (2006) 1115-21.

[42] P. Grieco, A. Carotenuto, P. Campiglia, I. Gomez-Monterrey, L. Auriemma, M. Sala, C. Marcozzi, R. d'Emmanuele di Villa Bianca, D. Brancaccio, P. Rovero, P. Santicioli, S. Meini, C.A. Maggi, E. Novellino, New insight into the binding mode of peptide ligands at Urotensin-II receptor: structure-activity relationships study on P5U and urantide, Journal of medicinal chemistry 52(13) (2009) 3927-40.

[43] D. Brancaccio, A. Limatola, P. Campiglia, I. Gomez-Monterrey, E. Novellino, P. Grieco, A. Carotenuto, Urantide conformation and interaction with the urotensin-II receptor, Archiv der Pharmazie 347(3) (2014) 185-92.

[44] A. Carotenuto, P. Grieco, P. Campiglia, E. Novellino, P. Rovero, Unraveling the active conformation of urotensin II, Journal of medicinal chemistry 47(7) (2004) 1652-61.

[45] S.M. Cowell, Y.S. Lee, J.P. Cain, V.J. Hruby, Exploring Ramachandran and chi space: conformationally constrained amino acids and peptides in the design of bioactive polypeptide ligands, Curr Med Chem 11(21) (2004) 2785-98.

[46] B.K. Kobilka, X. Deupi, Conformational complexity of G-protein-coupled receptors, Trends Pharmacol Sci 28(8) (2007) 397-406.

[47] S. Miura, Y.H. Feng, A. Husain, S.S. Karnik, Role of aromaticity of agonist switches of angiotensin II in the activation of the AT1 receptor, J Biol Chem 274(11) (1999) 7103-10.

FIGURE LEGENDS

Figure 1. Structures of the non-natural amino-acids introduced at position 6 in URP. Phe(pI), para-iodo-phenylalanine; Bip, biphenylalanine; Pep, (phenylethynyl)-phenylalanine; Phg, phenylglycine; Tic(7-OH), 7-hydroxy-1,2,3,4-tetrahydroisoquinoline.

Figure 2. Displacement curves of [^{125}I]URP binding for the different peptides of the library on CHO-UT cells. Data represent the mean ± S.E.M. of three independent experiments each performed in duplicate.

Figure 3. Representative concentration-response curves obtained with rat thoracic aorta rings after adding cumulative concentrations of URP or its analogs. Efficacy is expressed as a percentage of the amplitude of the contraction induced by KCl (40 mM). Each replicate (n) was conducted on tissue from at least 3 different animals. Data represent the mean ± S.E.M.

Figure 4. Agonist properties of URP and its analogs on the Gq activation using a BRET-based biosensor. Efficacy is expressed as a percentage of the URP maximal response (10^{-5} M). Data represent the mean ± S.E.M. of three independent experiments each performed in duplicate.

Figure 5. Agonistic properties of URP and its analogs on the G_{12} activation using a BRET-based biosensor. Efficacy is expressed as a percentage of the URP maximal response (10^{-5} M). Data represent the mean ± S.E.M. of three independent experiments each performed in duplicate.

Figure 6. Representative concentration-response curves obtained with rat thoracic aorta rings after adding cumulative concentrations of URP or UII following a pre-treatment with [Pep^6]URP (3.10^{-8} M). Efficacy is expressed as a percentage of the amplitude of the contraction induced by KCl (40 mM). Each replicate (n) was conducted on tissue from at least 3 different animals. Data represent the mean ± S.E.M.

Graphical abstract. Tyr residue of URP is crucial for UT activation. [Pep^6]URP, which is 10-times more efficacious at G_{12} activation compared to Gq, can discriminate the vasocontractile action of UII and URP.

Table 1. Amino acid sequences and analytical data of URP and its related analogs.

Peptide	*Sequence*	*Calculated*[a]	*Observed*[a]
URP	H-Ala-[Cys-Phe-Trp-Lys-Tyr-Cys]-Val-OH	1016.4	1017.1
[Phe(pI)^6]URP	H-Ala-[Cys-Phe-Trp-Lys-Phe(pI)-Cys]-Val-OH	1126.3	1127.7
[Bip^6]URP	H-Ala-[Cys-Phe-Trp-Lys-Bip-Cys]-Val-OH	1076.5	1078.5
[Pep^6]URP	H-Ala-[Cys-Phe-Trp-Lys-Pep-Cys]-Val-OH	1100.5	1101.8
[D-Phe(pI)^6]URP	H-Ala-[Cys-Phe-Trp-Lys-***Phe(pI)***-Cys]-Val-OH	1126.3	1127.1
[D-Bip^6]URP	H-Ala-[Cys-Phe-Trp-Lys-***Bip***-Cys]-Val-OH	1076.5	1077.4
[D-Pep^6]URP	H-Ala-[Cys-Phe-Trp-Lys-***Pep***-Cys]-Val-OH	1100.5	1101.8
[Tic(7-OH)^6]URP	H-Ala-[Cys-Phe-Trp-Lys-Tic(7-OH)-Cys]-Val-OH	1028.4	1030.0
[Phg^6]URP	H-Ala-[Cys-Phe-Trp-Lys-Phg-Cys]-Val-OH	986.4	986.6

[a]MALDI mass spectral analysis (m/z). The observed m/z of the monoisotope compared with the calculated monoisotopic mass. D-amino acids are indicated in bold italic letters.

Table 2. Binding affinity and contractile activity of URP and related analogs.

	Binding affinity		Aortic ring contraction		
Peptide	n	pIC_{50}	n	E_{max}[a]	pEC_{50}
URP	6	7.64 ± 0.09	19	116 ± 4	8.11 ± 0.06
[Phe(pI)^6]URP	4	8.25 ± 0.10**	4	95 ± 7*	8.12 ± 0.20
[Bip^6]URP	3	8.19 ± 012**	4	105 ± 8	7.50 ± 0.18***
[Pep^6]URP	3	7.70 ± 0.09	3	98 ± 5	6.77 ± 0.10***
[D-Phe(pI)^6]URP	3	5.46 ± 0.16***	4	61% @ 10 µM	
[D-Bip^6]URP	3	<5***	3	7% @ 10 µM	
[D-Pep^6]URP	3	5.82 ± 0.08***	5	34% @ 10 µM	
[Tic(7-OH)^6]URP	3	6.11 ± 0.11***	5	52 ± 5***	6.53 ± 0.20***
[Phg^6]URP	4	6.45 ± 0.22***	4	37 ± 12***	6.24 ± 0.49***

[a]Maximum efficacy is expressed as a percentage of the amplitude of the contraction induced by KCl (40 mM). All values are expressed as mean ± SEM. Statistical analysis was performed using an unpaired Student's t test, *$P \leq 0.05$, **$P \leq 0.01$, ***$P \leq 0.001$, versus values obtained for URP. Each replicate (n) was conducted on tissue from a different animal or on a different cellular passage.

Table 3. Gq and G_{12} activation by URP and related analogs.

	Gq activation			G_{12} activation			G_{12}/Gq activation bias[b]
Peptide	n	E_{max}[a]	pEC_{50}	n	E_{max}[a]	pEC_{50}	$10^{\Delta\Delta\log(\frac{\tau}{KA})}$
URP	4	100 ± 5	8.03 ± 0.18	5	100 ± 5	7.43 ± 0.15	1.00 ± 1.32
[Phe(pI)^6]URP	6	92 ± 5	7.85 ± 0.17	5	92 ± 6	7.57 ± 0.20	1.51 ± 1.31
[Pep^6]URP	5	99 ± 6	6.84 ± 0.16 **	5	90 ± 6	7.32 ± 0.17	9.95 ± 1.42 **
[D-Bip^6]URP	3	Inactive		5	Inactive		Inactive
[Tic(7-OH)^6]URP	4	61 ± 6**	7.00 ± 0.24 **	5	98 ± 7	6.73 ± 0. 18 *	22.13 ± 1.51 ***

[a]Maximum efficacy is expressed as a percentage of the activation induced by URP (10^{-5}M). [b]Bias was calculated using the Black-Leff operational model and URP was used as the reference (unbiased) ligand. All values are expressed as mean ± SEM. Statistical analysis was performed using an unpaired Student's t test, $*P \leq 0.05$, $**P \leq 0.01$, $***P \leq 0.001$, versus values obtained for URP. Each replicate (n) was conducted on a different cellular passage.

Table 4. Antagonistic contractile activity of [Pep^6]URP.

Peptide	Aortic ring contraction hUII			Aortic ring contraction URP		
	n	E_{max}	pEC_{50}	n	E_{max}	pEC_{50}
No treatment	15	102 ± 4	8.52 ± 0.11	19	116 ± 4	8.11 ± 0.06
[Pep^6]URP 3.10^{-8} M	3	96 ± 3	8.11 ± 0.12 *	3	73 ± 5 ***	7.30 ± 0.24 ***

[a]Maximum efficacy is expressed as a percentage of the amplitude of the contraction induced by KCl (40 mM). Aortic rings were pre-treated with [Pep^6]URP for 30 minutes prior UII or URP treatment. All values are expressed as mean ± SEM. Statistical analysis was performed using an unpaired Student's t test, $*P \leq 0.05$, $**P \leq 0.01$, $***P \leq 0.001$, versus values obtained for URP. Each replicate (n) was conducted on tissue from a different animal.